ST-ECF Instrument Science Report WFC3-2005-17

Ground tests of the WFC3 UVIS grism

S. S. Larsen, H. Bushouse, J. R. Walsh
March 2005

ABSTRACT

The fundamental parameters of a slitless dispersing element are the geometrical configuration of the spectral orders, the dispersion relation relating pixel offset to wavelength and the sensitivity of each order. Based on ambient and thermal vacuum tests, the performance of the WFC3 UVIS G280L grism has been assessed. The locations of the different orders relative to exposures taken through a direct imaging filter are determined, wavelength solutions are derived, and the relative throughput of the different orders is quantified. The wavelength solution was found to be a nearly linear function of pixel offset for all orders and the tilt of the spectra to the pixel grid is 3 degrees, but the orders are curved. However the G280L grism shows a very high concentration of flux in the zeroth order, which only has very small spectral dispersion, and as a result the fraction of incident flux in the 1st order is only ~30% over the full wavelength range 200 nm - 500 nm. Only from 200 nm - 300 nm does the 1st order receive more flux than the 0th order.

1. Introduction

The Wide Field Camera 3 is fitted with three grisms for slitless spectroscopy. In the UVIS channel there is one grism G280L for the near-UV - visible range, which was originally a WFPC1 flight spare grism. The NIR channel has two grisms for the shorter and longer NIR wavelengths. The fundamental design parameters of a grism are the deflection of the incident beam by the grism (defined by the prism angle), dispersion in the various orders and the energy in each order (its sensitivity). In order to extract slitless spectra from grism images it is necessary to know these paraemters and how they vary with position in the field. With a good parameterization, then extraction software, such as the aXe task developed at the ECF (http://www.stecf.org/~aXe), can be applied to extract multiple slitless spectra from sky images.

During the ground ambient and Thermal Vacuum (TV) testing of WFC3 in 2004, specific tests for the grisms were included. Test UVIS24 was designed to allow determination of the dispersion of the UVIS G280L grism through illumination by a monochromator of a pinhole (5micron point target). The design band width of the monochromator was 10nm. It was planned to obtain the narrowband spectra at five apertures over the UVIS field. In

conjunction with these monochromator measurements, a dispersed white light spectrum would be taken at a few positions, in order to map the spectrum tilt and trace. This ISR describes the implementation of this test and the analysis of the results. Tables provide the details of the spectral trace and the dispersion solution. Some conclusions on the likely problems to be encountered through use of this grism in-orbit are provided.

2. Test set-up

The UV24S01 grism test was executed on WFC3 on June 30, 2004 with WFC3 in an ambient environment and again on October 1, 2004 under thermal-vacuum conditions. For the June 30 run, the WFC3 was located in the Spacecraft Systems Development and Integration Facility (SSDIF) at Goddard Space Flight Center (GSFC), which is an ambient environment clean room. For the October 1 test, WFC3 was installed in a Space Environment Simulator (SES) chamber at GSFC, where it was operated under flight-like thermal-vacuum conditions. On both occasions, the WFC3 external optical stimulus system, CASTLE, was used to provide the necessary source targets for the grism tests.

When WFC3 is operated in an ambient environment, the optical bench components (and hence the grisms) are at room temperature and the UVIS channel CCD detector is operated at a temperature of -70^{o} C. For the June execution of the grism test the UVIS filter mechanism temperature was consequently ~24^{o} C. For the October execution of the test, when WFC3 was in a thermal-vacuum environment, the filter mechanism was at -1.8^{o} C and the UVIS CCD detectors were at -82^{o} C.

Each UVIS24 test run included two sets of point-source exposures, one with the target located near the center of the UVIS channel field of view and the other with the target near a corner of the field, in order to investigate the effects of geometric distortion on the grism dispersion parameters. All exposures used the CASTLE Xenon source lamp, with a 5 μm pinhole used to provide an unresolved target.

Table 1. *Log - June 2004, ambient tests. The reference positions (i.e. the images of the continuum beam in F300W) for Chip1 and Chip2 are at (X_{ref},Y_{ref}) = (1966.14, 167.42) = UV02 target and (3773.68, 259.37) = UV11 target, respectively.*

Filename	Grating/Filter	Chip	Lambda centre (nm)	Lambda width (nm)	Exptime (s)
iu240101r_04182135719	F300W+ND2	1	Cont.	-	3
iu240102r_04182135719	G280L+ND2	1	Cont.	-	3
iu240104r_0418214253t	G280L	1	200	10	400
iu240105r_04182142537	G280L+ND1	1	230	10	50
iu240107r_04182144701	G280L+ND2	1	260	10	30
iu240108r_04182144701	G280L+ND2	1	290	10	55
iu24010ar_04182150713	G280L+ND2	1	320	10	12
iu24010br_04182150713	G280L+ND2	1	350	10	10
iu24010dr_04182152713	G280L+ND2	1	380	10	10
iu24010er_04182152713	G280L+ND2	1	410	10	10
iu24010gr_04182154652	G280L+ND2	1	440	10	10
iu24010hr_04182154652	G280L+ND2	1	470	10	10
iu24010jr_04182161218	G280L+ND2	1	500	10	10
iu24010kr_04182161218	F300W+ND2	2	Cont.	-	3
iu24010lr_04182161218	G280L+ND2	2	Cont.	-	3
iu24010nr_04182165544	G280L	2	200	10	400
iu24010or_04182165544	G280L+ND1	2	230	10	50
iu24010pr_04182165544	G280L+ND2	2	260	10	30
iu24010qr_04182165544	G280L+ND2	2	290	10	55
iu24010sr_04182172817	G280L+ND2	2	320	10	12
iu24010tr_04182172817	G280L+ND2	2	350	10	10
iu24010ur_04182172817	G280L+ND2	2	380	10	10
iu24010vr_04182172817	G280L+ND2	2	410	10	10
iu24010xr_04182175449	G280L+ND2	2	440	10	10
iu24010yr_04182175449	G280L+ND2	2	470	10	10
iu24010zr_04182175449	G280L+ND2	2	500	10	10

Table 2. *Log - October 2004, thermal vacuum tests. The reference positions for Chip1 and Chip2 are at (X_{ref},Y_{ref}) = (1984.60, 147.90 - UV02 target) and (3789.99, 238.47 - UV11 target)*

Filename	Grating/Filter	Chip	Lambda centre (nm)	Lambda width (nm)	Exptime (s)
iu24a101r_04275010606	F300W+ND1	1	cont.	-	2
iu24a102r_04275010606	G280L+ND1	1	cont.	-	3
iu24a103r_04275013557	G280L	1	200	10	600
iu24a105r_04275013557	G280L	1	230	10	50
iu24a106r_04275013557	G280L	1	260	10	30
iu24a107r_04275013557	G280L	1	290	10	30
iu24a109r_04275020552	G280L	1	320	10	10
iu24a10ar_04275020552	G280L	1	350	10	10
iu24a10br_04275020552	G280L	1	380	10	10
iu24a10cr_04275020552	G280L	1	410	10	10
iu24a10er_04275023816	G280L	1	440	10	10
iu24a10fr_04275023816	G280L	1	470	10	10
iu24a10gr_04275023816	G280L	1	500	10	10
iu24a10hr_04275023816	F300W+ND1	2	cont.	-	2
iu24a10jr_04275025602	G280L+ND1	2	cont.	-	3
iu24a10kr_04275032553	G280L	2	200	10	600
iu24a10mr_04275032553	G280L	2	230	10	50
iu24a10nr_04275032553	G280L	2	260	10	30
iu24a10or_04275032553	G280L	2	290	10	30
iu24a10qr_04275035548	G280L	2	320	10	10
iu24a10rr_04275035548	G280L	2	350	10	10
iu24a10sr_04275035548	G280L	2	380	10	10
iu24a10tr_04275035548	G280L	2	410	10	10
iu24a10vr_04275043013	G280L	2	440	10	10
iu24a10wr_04275043013	G280L	2	470	10	10
iu24a10xr_04275043013	G280L	2	500	10	10
iu24a10yr_04275043013	ND2	1	350	10	3
iu24a110r_04275044551	G280L+ND2	1	350	10	3

3. Measurements

Logs of the test exposures of the two test sessions are given in Tables 1 and 2 respectively. During each test run, a series of monochromatic exposures (with a bandwidth of 10 nm) were obtained through the G280L grism at wavelengths from 200 nm - 500 nm in steps of 30 nm. For each run, only two test series were obtained on account of time constraints. One series was with the spectra placed near the bottom of Chip 1 (target UV02 i.e. near the geometric center of the WFC3 UVIS field of view) and another near the bottom right corner of Chip 2 (target UV11). This approach allows a first-order assessment of any field dependence of the spectral traces and wavelength solution. In addition to the monochromator exposures, spectra of a continuum source and direct images of the beam through the F300W filter were also obtained at the same positions. During the first (ambient) test run, neutral density (ND) filters were inserted into the beam during the monochromator exposures, while the ND filters were used only for the continuum source exposures during the TV tests. The last two images taken during the TV test run used a CASTLE 200 micron diameter fibre (as opposed to a point source), which provides an extended source for more reliable absolute flux measurements.

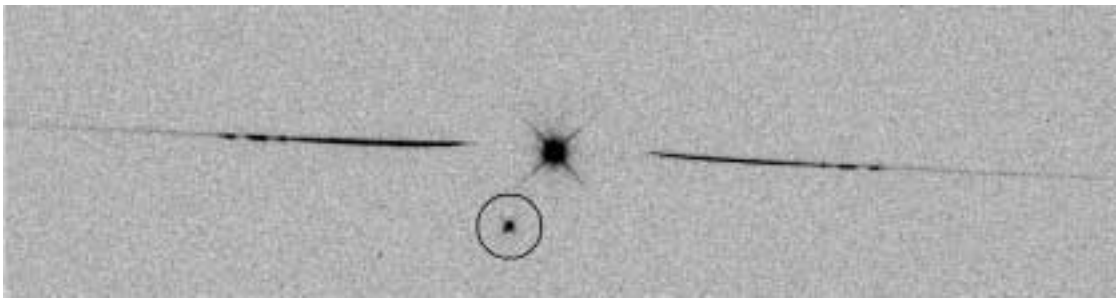

Figure 1: *Sum of a direct image taken through the F300W filter (marked with a circle) and the G280L spectrum of a continuum source. Note the dominating 0th order, the significant offset between the direct image and the spectra, and the curvature of the +/-1st order spectral traces near their blue end.*

Figure 1 shows the sum of the G280L continuum spectra and the corresponding F300W direct image for Chip 1 (from the TV tests). Only a 3200x900 pixels subsection of the chip is shown here. The prominent feature near the center of the figure is the 0th order, with the +1st and -1st orders extending towards the left and right, respectively. The +1st order is taken to be that with the higher throughput and happens to lie to lower X pixels than the position of the 0th order. The direct image is marked by a circle. One notes a substantial offset (about 170 pixels) in the y-direction between the direct image and the spectra, and significant curvature near the blue ends of the +/-1st orders.

4. Analysis

The datasets containing spectra, listed in Tables 1 and 2, were analysed. The bias was subtracted from the images, the orders were traced and dispersion solutions fitted to the measured positions of the monochromator spots versus wavelength as listed in column 4 of Tables 1 and 2.

Tracing the spectral orders

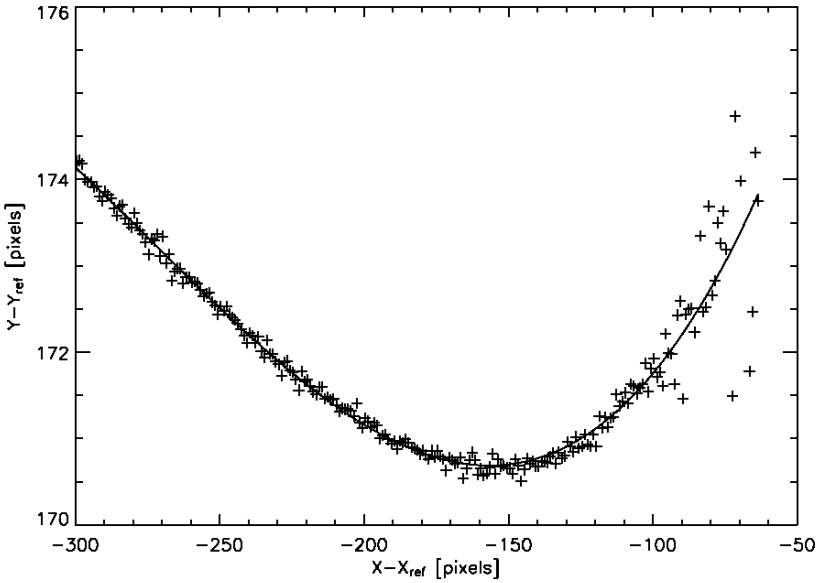

Figure 2: *Trace of the +1st order and the best-fitting 3rd order polynomial*

The ST-ECF aXe package for reduction of slitless spectroscopy data treats the spectral traces and wavelength solutions defined with respect to the position of the source in the direct image. The centroid of the continuum source image in the F300W exposures (X_{ref}, Y_{ref}) was determined by running SExtractor. This position was assumed not to change through the duration of the measurements.

For the data obtained during the June 2004 ambient test run, only the +1st, +2nd, 0th and -1st orders could be clearly identified. However, for the October 2004 TV test data (where no ND filters were used) the S/N was much higher and at least 8 positive and 8 negative orders were visible (Figure 4), although we will limit most of our discussion in this report to the +/-4 lowest orders. As a crude first estimate, the extent along the trace of the different spectral orders was then determined by measuring the X-position of the monochromator spots in the shortest- and longest wavelength grism exposures.

For the +/-1st orders, the spectra were traced by measuring the centroid across the spectra of the continuum source and fitting a 3rd order polynomial to ($Y-Y_{ref}$) vs ($X-X_{ref}$). Here, ($Y-Y_{ref}$) is the offset along the CCD columns between the trace centroid and the source position in the direct image, and ($X-X_{ref}$) is the offset along the CCD x-axis (roughly parallel to the dispersion direction). The ($Y-Y_{ref}$) offsets and the best-fitting polynomial for the +1st order are shown in Fig. 2 for the CHIP1 data from the thermal vacuum (October 2004) test series. The centroids were measured with a custom-written C-program. For the 2nd-4th orders, a common 2nd-order polynomial was used to fit all the spectral traces, although inspection of the monochromator spectra shows that the bend at the blue end is present also in the higher-order spectra (and even in the 0th order, see Figure 3). In fact, the offset in the y-direction (relative to the common trace definition) seen at short wavelengths appears to be similar for all orders when expressed in pixel units, suggesting a slight dispersion in the y-direction by the G280L grating. The coefficients for the trace fits and the approximate X-range of each order are listed in Table 3. As can be seen from the coefficients listed in the table (and Figure 4), the overall dispersion direction has only a slight tilt with respect to the CCD x-axis (about -3 deg).

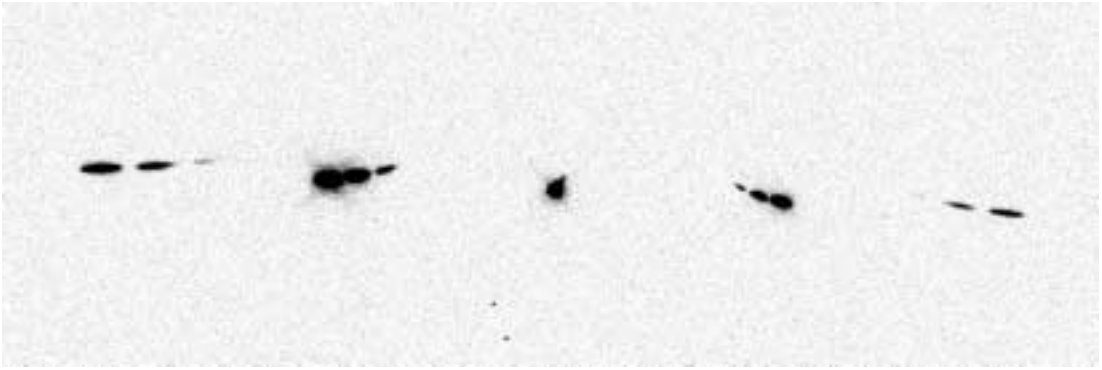

Figure 3: *Sum of the 200 nm, 230 nm and 260 nm G280L spectra, showing the orders 2, 1, 0, -1 and -2. The bending of the spectral traces, particularly at the blue end is clearly noticable.*

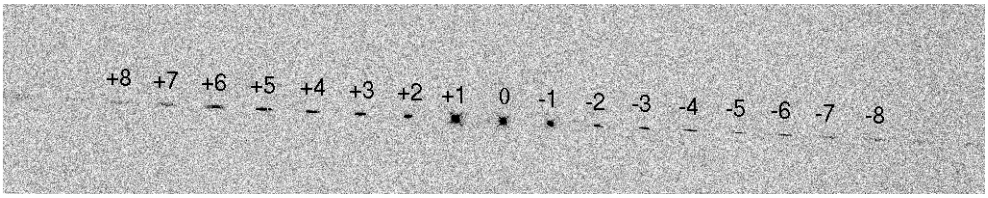

Figure 4: *Section of a G280L exposure on Chip 1 for the 290 nm monochromator setting from the thermal vacuum test series. Orders from -8 to +8 are labeled.*

Table 3. *Trace descriptions for orders -4 to +4 for the ambient and TV tests. The traces are fit by polynomials of the form (Y-Y_{ref}) = DYDX_0 + DYDX_1*(X-X_{ref}) + DYDX_2*(X-X_{ref})^2 + ..., where (X_{ref},Y_{ref}) is the position of the source in the direct image. Columns 2-4 are for Chip 1 and Columns 5-7 are for Chip 2.*

Order	(X-X_{ref}) range	DYDX*	FWHM (y, @290 nm)	(X-X_{ref}) range	DYDX*	FWHM (y, @290 nm)
Ambient						
+1	-300 .. 0	1.8034E02 1.3350E-01 4.8675E-04 4.6410E-07	2.9	-300..0	1.7091E02 1.2702E-01 4.3299E-04 4.0294E-07	2.6
0	60..120	155.7	2.4	60..120	148.51	2.9
-1	150..630	2.2055E02 -3.5846E-01 5.5428E-04 -3.2551E-07	2.1			3.3
Thermal Vac.						
0	60..120	155.7	2.6	60..120	148.5	2.8
+1	-300..0	1.8088E02 1.5055E-01 6.7517E-04 8.2767E-07	3.2	-300..0	1.7384E02 1.8050E-01 7.9532E-04 1.0324E-06	2.3
-1	150..630	2.2988E02 -4.2861E-01 6.8362E-04 -4.1553E-07	2.2			
2..4,-2..-4		1.619E02 -4.940E-02 9.587E-08				
2..4					1.5340E02 -4.0737E-02 -6.8996E-07	
+2	-650..-150		4.4			2.6
-2	300..820		2.2			
+3	-1000..-240		5.7			3.1
-3	450..1170		2.7			
+4	-1400..-350		7.2			4.2
-4	570..1520		3.5			
	Chip 1	Chip 1	Chip 1	Chip 2	Chip 2	Chip 2

Dispersion solutions

The trace definitions were inserted into a configuration file for the aXe spectral extraction software and each of the monochromator spectra was then extracted using the standard aXe tasks (SEX2GOL, GOL2AF, AF2PET, BACKEST, STAMPS and PET2SPC). These tasks extract a number of "beams" corresponding to individual spectral orders, using the location of the beams with respect to the object position in the direct image as specified in the aXe configuration file. The STAMPS task produced stamp images which allowed us to visually verify that the correct spectra were extracted, and PET2SPC produced output spectra in FITS binary table format. A wide extraction box extending to +/-20 pixels on both sides of the trace was used, thus including most of the flux even from the higher orders which were somewhat out of focus (see below). The FITS spectra produced by aXe were then converted to IRAF format (using the TDUMP and RSPECT tasks in IRAF) and the $(X\text{-}X_{ref})$-location of the peak of each monochromator spot was measured by carrying out a Gaussian fit to the extracted spectrum using the SPLOT task in the ONEDSPEC package in IRAF.

The wavelength solutions are well approximated by linear fits, with the coefficients listed in Table 4. While quadratic fits did yield statistically significant second-order terms (at least for the 1st and 2nd orders), the difference between linear and quadratic dispersion solutions generally amounted to less than about +/-1 nm over the 200-500 nm wavelength range. The one exception was the -1st order, for which some curvature was evident and the deviations from a straight line here were as large as +/-3 nm. If an accurate wavelength calibration is desired then it may be worthwhile to include second-order terms, but here only linear fits were performed. The fits to the first 4 positive orders are illustrated in Figure 5.

The wavelength solutions hold no major surprises. The +1st and -1st orders have dispersions of about -1.4 nm/pixel and +1.6 nm/pixel, with the +/-2nd, +/-3rd and +/-4th orders having dispersions of about 1/2, 1/3 and 1/4 the +/-1st order dispersions respectively, as expected. The 0th order also has some dispersion, about -50 nm/pixel. There is some field dependence, with the +1st order dispersion varying by about 5% between the field center and the corner (on Chip 2). At wavelengths longer than about 450 nm the +1st order is contaminated by the blue end (lambda<260nm) of the +2nd order. Higher orders show even more overlap (see Figure 5).

As can be seen in Figure 3, the 10 nm bandwidth of the monochromator is not negligible. Indeed, the FWHM values measured from the Gaussian fits to the monochromator spots are about 9, 17, 25 and 33 pixels for the +/-1st to +/-4th orders, corresponding to roughly 12 nm in all cases. Including a modest contribution due to broadening by the point spread

function, these FWHM values are then in good agreement with the expected broadening due to the finite bandwidth of the monochromator.

Table 4. *Wavelength solutions for the -4th to +4th orders. The wavelength solutions are approximated by linear fits of the form Lambda (nm) = DLDP_0 + DLDP_1 * (X-X_{ref}), where X_{ref} is the X-coordinate of the source in the direct image. Columns 2-3 list the solutions for Chip 1, and columns 4-5 give the solutions for Chip 2*

Order	**DLDP_0**	**DLDP_1**	**DLDP_0**	**DLDP_1**
Ambient				
0	5.137E03	-5.001E01	5.797E03	-5.759E01
+1	1.479E02	-1.418E00	1.527E02	-1.480E00
-1	-1.858E02	1.564E00		
+2	7.074E01	-7.333E-1		
Thermal Vac				
0	5.264E03	-5.032E01	4.697E03	-4.538E01
+1	1.524E02	-1.412E00	1.544E02	-1.480E00
-1	-1.943E02	1.568E00		
+2	7.536E01	-7.228E-01	7.671E01	-7.573E-01
-2	-8.241E01	7.572E-01		
+3	5.287E01	-4.793E-01	5.383E01	-5.020E-01
-3	-5.637E01	5.041E-01		
+4	4.094E01	-3.586E-01	4.132E01	-3.762E-01
-4	-4.296E01	3.778E-01		
	Chip 1	Chip 1	Chip 2	Chip 2

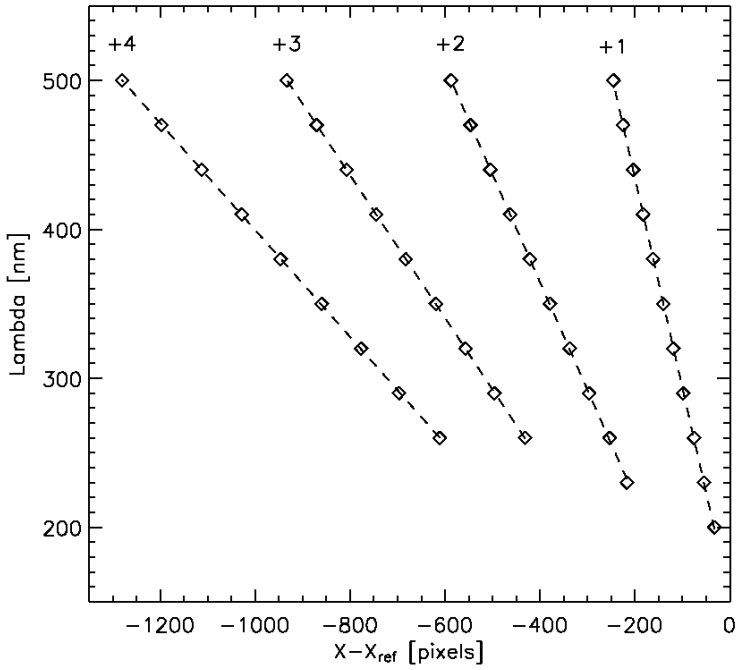

Figure 5: *Wavelength solutions for orders +1 to +4. Note the overlap between the higher orders. Measured points are shown by circles and the fitted dispersion solutions, from Table 4, by dashed lines.*

Flux in different orders

The relative throughput of the different orders was estimated by measuring the counts in circular apertures with radii of 50 pixels, centered on each order, on the monochromator spectra. Figure 6 shows the flux in orders -4..+4, normalized to the total flux in all orders, for the wavelength range 200 nm - 500 nm. As was already noted in the discussion of Figure 1, a large fraction of the flux is contained within the 0th order which actually dominates at wavelengths longer than 320 nm. At 500 nm, about 70% of the total flux is in the 0th order. The flux in the -1st order varies between 20% and 60% of that in the +1st order over the wavelength range.

Table 5 lists the relative flux in different orders summed over the wavelength range 200nm - 500 nm (based on the monochromator spectra). The table again shows that a large fraction, about half, of the flux is in the 0th order, but with significant contributions (about 1%) even from the +/-3rd orders.

In order to further quantify the throughput, we used the spectra and direct images which were obtained for a monochromator beam setting of 350 nm during the thermal vacuum test run. A neutral density (ND2) filter was employed for both the spectroscopic and direct imaging exposures. Figure 7 shows the measured flux in orders -8..+8, relative to the flux in the direct image. At 350 nm the throughput of the 0th order is about 40% relative to the direct image, while the throughput in the +1st order is about 27%.

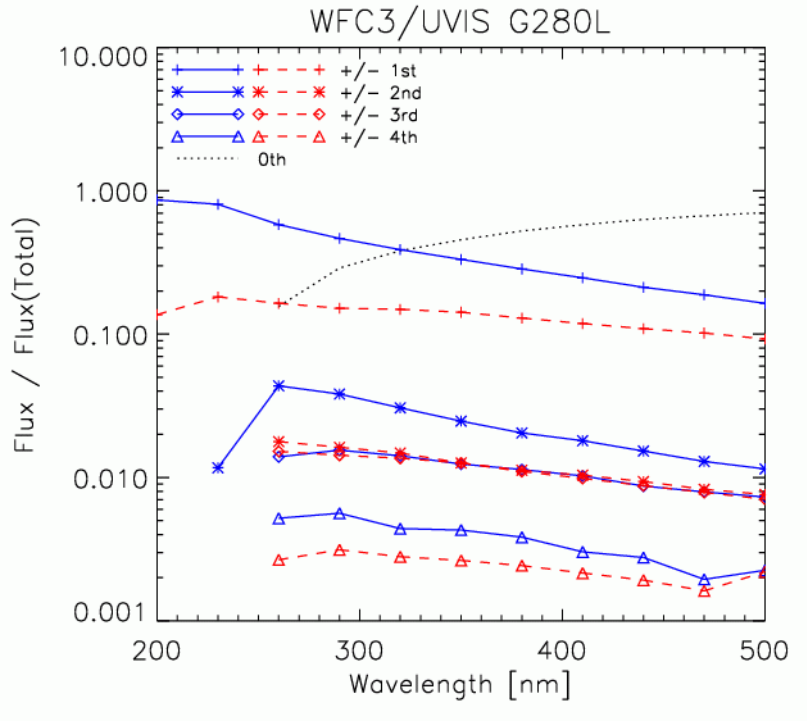

Figure 6: *The flux measured in orders 0..+/-4, relative to the total flux in all orders, as a function of wavelength. Positive and negative orders are shown with solid blue and dashed red lines, respectively.*

Table 5. *Flux in different orders relative to the total flux, summed over the wavelength range 200..500 nm.*

Order	Flux/Total
0	0.49
+1	0.32
+2	0.023
+3	0.011
+4	0.004
-1	0.13
-2	0.012
-3	0.011
-4	0.002

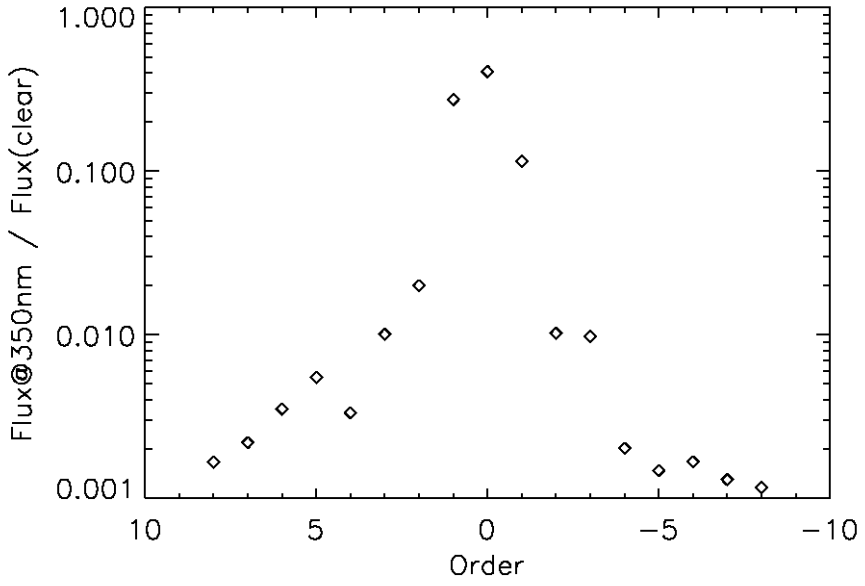

Figure 7: *Measured flux in orders -8..+8 relative to a direct image is shown for a monochromator setting of 350 nm.*

Focus variations

Table 3 also lists the FWHM measured in the y-direction for each order (-4..+4) on the 290 nm spectrum. As a reference, the FWHM in the direct image of the continuum source is

about 2.2 pixels. We note that the +1st order appears slightly broadened in both test runs, although this effect is less pronounced for the Chip 2 exposures. Also, the 0th and -1st orders appear slightly narrower than the +1st order.

A more detailed comparison is given in Figure 8, which shows the FWHM measured along the CCD Y-axis for orders -4..4, using the Chip 1 test series from the TV test run. This is the only test series which allows full characterization of all positive and negative orders. It is again clear that the negative orders tend to be somewhat more sharply defined than the positive ones, with all orders (except perhaps the -1st) being significantly broader than the FWHM measured on the direct image

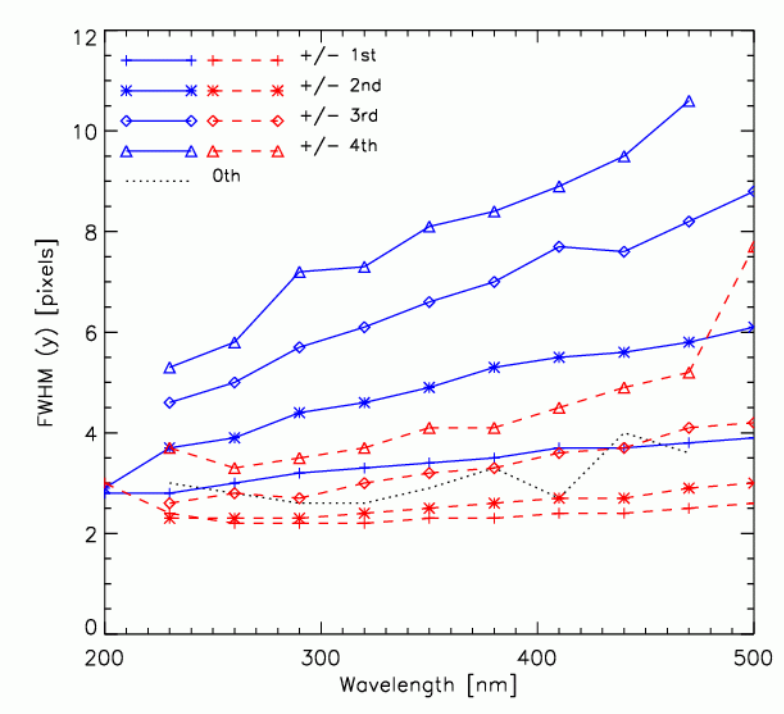

Figure 8: *Full Width at Half Maximum measured along the y-direction for spectral orders -4..+4 is shown as a function of wavelength. Positive and negative orders are shown with solid blue and dashed red lines, respectively.*

5. Conclusions

Ground tests at ambient temperature and in vacuo were conducted to measure the traces and the dispersion solutions for the orders of the WFC3 UVIS G280L grism. The dispersion is close to linear in all orders and in the stronger first order the dispersion is 1.4nm/

pixel. The deficiency of this grism is however that the amount of energy in the zeroth order, which only has a dispersion of 50nm/pixel, is large and amounts to about 50% over the wavelength range 200 to 500nm. The +1st order, which is assumed to be that most useful for scientific spectroscopy, only receives about 30% of the total flux over the total wavelength range. Over the wavelength range 200 nm - 300 nm the 1st order does receive most of the flux, making the UVIS grism most useful for observations over this restricted wavelength range. If high spatial resolution is critical, observers might consider relying on the -1st order which appears to produce somewhat sharper spectra than the +1st order. The resultant slitless spectra of crowded fields will however be dominated by the zeroth order spectra and bright objects will badly contaminate adjacent spectra, since the flux in higher orders is also significant.

Acknowledgements

We thank W. Freudling for a number of helpful comments.